

Implementation and Analysis of the Decomposition-Fusion ECCM Technique

Benjamin J. Slocumb^a and Philip D. West^a and X. Rong Li^b

^aGeorgia Tech Research Institute, Georgia Institute of Technology, Atlanta, GA 30332-0840, USA

^bDepartment of Electrical Engineering, University of New Orleans, New Orleans, LA 70148, USA

ABSTRACT

In a previous paper,¹ the authors proposed a new general and systematic electronic counter-countermeasure (ECCM) technique called the Decomposition and Fusion (D&F) approach. This ECCM is implemented within the multiple target-tracking framework for protection against range-gate-pull-off (RGPO) and range false target ECM techniques. The original formulation left open the specific multiple target tracking framework. In this paper, we develop a specific implementation of the D&F technique and evaluate it within the Benchmark 2 Problem²⁻⁴ environment. Simulation results are presented showing the track-loss rejection capabilities and the track accuracy performance of the D&F technique.

Keywords: Electronic Counter-countermeasures, Range-Gate-Pull-Off, Data Fusion, Target Tracking

1. INTRODUCTION

Many modern military units possess electronic countermeasure (ECM) systems that produce radio frequency (RF) jamming waveforms for the purpose of disruption or deception of an enemy tracking radar system. ECM is primarily used to protect friendly aircraft (and some ships and ground units) from threat radar systems that might deploy radar-guided weapons against the platform. The goal of the ECM is to prevent or delay target tracking or to cause track loss once tracking is initiated. When the ECM is effective against the tracking radar, launch of a radar-guided weapon can be prevented or delayed, or the ECM causes launched missiles to miss the target. Successful jamming is accomplished by preventing target detection, causing the radar to incorrectly start a track, causing large track errors and/or track loss, or by overloading the tracker with false measurements.

The need to consider ECM during target tracking algorithm development was demonstrated at the 1995 American Control Conference.² As an invited special session, several research groups were asked to develop target tracking algorithms for a standardized radar system model and then to test their algorithms using a common set of trajectories for maneuvering military targets. Two types of ECMs were included in the Benchmark 2 problem: standoff noise jamming and self-protection range-gate-pull-off (RGPO). The results indicated that some tracking algorithms performed well in the presence of ECM, while others⁵ were extremely vulnerable (i.e., the tracker frequently lost track due to the ECM). The RGPO countermeasure presents a difficult problem because it is a *deception* technique that cannot simply be overcome by increasing the radar transmit power or by nulling the jamming signal. Since a RGPO false target looks identical to credible radar echo, it must be modeled within the target tracking algorithm.

Our previous paper¹ formulated a range false target rejection scheme based on a rigorous framework called *Decomposition and Fusion Anti-RGPO* (D&F-ARGPO). The technique has four fundamental components: (a) decomposing the validated measurements by determination of range deception measurements using hypothesis testing; (b) running one or more tracking filters using the detected true target plus range deception measurements only; (c) running a conventional tracking-in-clutter filter using the remaining measurements; (d) fusing the tracking filters by a probabilistically weighted sum of their estimates. The D&F-ARGPO formulation is general, and we left open the specific multiple target tracking framework. The objective of this paper is to develop a specific implementation and evaluate it within the Benchmark 2 Problem²⁻⁴ environment. The implementation uses a special single-measurement filter that merges the target and false target measurement pair, while the remaining measurements are processed using the Strongest Neighbor (or PDAF) filter.

Other author information: Send correspondence to BJS: Email: ben.slocumb@gtri.gatech.edu; Telephone: 404-894-8239; Fax: 404-894-8636. XRL research supported by ONR Grants N00014-97-1-0570 and N00014-00-1-0677, NSF Grant ECS-9734285, and LEQSF Grant (1996-99)-RD-A-32.

2. THE RGPO PROBLEM

RGPO is a class of ECM that seeks to deceive the tracking radar in range. RGPO techniques are distinguished from other range false-target techniques in that they assume that the target is initially under track and that the tracker's range gate must be "pulled" off of the target (skin) return. Once the tracker is pulled off the true target, it is moved away in range and then "dropped" forcing the radar to reacquire the target. By forcing the radar to repeatedly reacquire the target, the radar can be prevented from reaching a track quality state necessary to launch a missile.

The RGPO technique is implemented by initially generating a false target that is coincident with the true target skin return. The ECM system may use a Cover Pulse (a wide pulse that overlaps the true target) to help obscure the actual range position. The amplitude of the false target may be set larger than that for the true target to make it more inviting. Next, the false target is walked-off the true target in range. This walk-off target is created by generating a delayed version of each radar pulse (the delay corresponds to the range translation). By varying the delay with time, the range position changes. Usually, the false target is walked in the outbound direction (range gate pull off). Against some radars the false target can be walked in the inbound direction (a range gate pull in), but this is not possible versus the Benchmark 2 Problem radar since it is an asynchronous single-pulse radar. Walk-off programs may include single or multiple walk-off targets. This work only considers a single false target (for simplicity and because the Benchmark 2 Problem simulation only supports a single false target).

Because of the way the RGPO false target is generated, it will be radially aligned with the true target but farther in range. Hence, the range deception measurements always come in pairs, one as the true target (or cover pulse if present) and the second as the false target. For convenience, we refer to this as the **target and false-target (target-FT) measurement pair**. A more comprehensive description of RGPO problem within the multiple target tracking context is given in Ref. 6, along with descriptions of other deception ECM techniques.

3. THE MEASUREMENT MODEL

At a given discrete time point t_k , a radar points the antenna at a particular bearing and elevation angle, say (\hat{b}_k, \hat{e}_k) . The radar transmits a pulsed waveform and any returned echos it receives are used to measure the target range. The ranging is accomplished by detecting energy in any of the range cells. Hence, multiple measurements can be obtained at a given time point. Let the set of measurements at time t_k be defined as

$$Z_k = [z_k^1, z_k^2, \dots, z_k^{M_k}] \quad (1)$$

The number of measurements M_k is less than or equal to the total number of range cells N_R . For the Benchmark radar, which is a 3D monopulse radar, the elements of each measurement vector z_k^i are

$$z_k^i = [r_k^i \quad b_k^i \quad e_k^i]' \quad (2)$$

$$= [\rho_k^t \quad \theta_k^t \quad \phi_k^t]' + w_k \quad (3)$$

where (r_k^i, b_k^i, e_k^i) are the measured range, bearing, and elevation values for the i th measurement, and $(\rho_k^t, \theta_k^t, \phi_k^t)$ are the true range, bearing, and elevation values of the target. Also, w_k represents zero-mean Gaussian measurement noise. The range measurement is in the set of quantized range bin values, with $dr = c\tau/2$ being the range resolution of the radar and τ being the compressed pulse width. In addition to the elements in z_k^i , the Benchmark radar will also return the estimated SNR, $\hat{\mathfrak{R}}_k^i$, and estimates of the azimuth and elevation error variance, $(\hat{\sigma}_{b_k^i}^2, \hat{\sigma}_{e_k^i}^2)$. As we will discuss below, these variance estimates reported by the radar are generated under the assumption that each measurement is a target (i.e., a different model applies for false alarms).

Each individual measurement can be physically classified as one of three types: a target, a false alarm, or a false target. Let z_k^t denote the target measurement during the radar dwell at time t_k . Let $z_k^{fa_i}$ denote the i th false alarm measurement on the dwell at time t_k . False alarms are due to thermal noise in the radar receiver. Let $z_k^{ft_i}$ be the i th false target measurement due to the RGPO deception ECM.

In the specific case of the Benchmark Problem RGPO false target, the measurement is given by $z_k^{ft_i} = [r_k^{ft_i}, b_k^t, e_k^t]$. The false target measurement has the same bearing and elevation as the true target (with different additive noise), but the range is $r_k^{ft_i} = r_k^t + \Delta r_k^i$. The range offset Δr_k is determined by the ECM program that creates the false target. By repeating the captured radar signal at the time delay time of Δt_k , the range offset is $\Delta r_k = c\Delta t_k/2$ based

on the two-way propagation expression. The Benchmark simulation is set up to create linear and parabolic range walk-off delays, which may be described as

$$\Delta t_k = \begin{cases} \frac{v_0(t_k - t_0)}{c}, & \text{Linear} \\ \frac{a_0(t_k - t_0)^2}{2c}, & \text{Parabolic} \end{cases} \quad (4)$$

where t_0 is the time of the start of the walk-off program, c is the speed of light, v_0 is the constant radial velocity of the linear walking false target, and a_0 is the constant radial acceleration of the parabolic walking false target.

4. SUMMARY OF THE MEASUREMENT DECOMPOSITION PROCEDURE

4.1. Statistical model of measurements

The first step in the D&F-ARGPO approach is to decompose the validated measurements into two sets: target-FT measurements and the remaining measurements. The measurement decomposition is accomplished by *detecting* the presence of and *isolating* any range deception measurements. The technique is based on a statistical hypothesis test of the received measurements. The test is formulated from statistical models of the different measurement types.

- **False Alarm.** The Benchmark radar is a monopulse radar. Accordingly, the bearing of a false alarm measurement has a Gaussian distribution: $b_k^{f a_i} \sim N(\hat{b}_k, \hat{\sigma}_{b_k: f a_i}^2)$ where \hat{b}_k is the bearing pointing angle of the radar. The radar reports a measurement variance, $\hat{\sigma}_{b_k: t_i}^2$, but this is not the variance for a false alarm. The estimated false alarm bearing variance is $\hat{\sigma}_{b_k: f a_i}^2 = 1/(2\hat{\mathfrak{R}}_k^i \kappa_{b_k}^2)$, and it is derived from equation (40) in Ref. 7 where the theoretical SNR is set to zero. $\hat{\mathfrak{R}}_k^i$ is the *observed SNR* reported by the radar (which in the case of a false alarm is just ratio of observed to theoretical noise power). The bearing monopulse slope³ is $\kappa_{b_k} = 48 \cos(\hat{b}_k)$. The elevation model for a false alarm follows an identical model, $e_k^{f a_i} \sim N(\hat{e}_k, \hat{\sigma}_{e_k: f a_i}^2)$. The elevation monopulse slope is $\kappa_{e_k} = 48 \cos(\hat{e}_k - e_{tilt})$, where the array face elevation tilt angle is $e_{tilt} = 15\pi/180$.
- **Target.** The bearing of a target measurement, $b_k^{t_i}$, has a Gaussian distribution with mean θ_k^t and variance $\hat{\sigma}_{b_k: t_i}^2$. In our model the target bearing variance is

$$\begin{aligned} \hat{\sigma}_{b_k: t_i}^2 &= [S_k|_{k-1}]_{22} \\ &= [H_k P_k|_{k-1} H_k']_{22} + \sigma_{b_k^i}^2 \end{aligned} \quad (5)$$

where $\hat{\sigma}_{b_k^i}^2$ is the (posterior) measurement variance produced by the radar signal processor from the measured received power in the target return, H_k is the Jacobian matrix in the EKF, and $P_k|_{k-1}$ is the predicted form of the state covariance matrix. The elevation measurement of the target, follows an identical statistical model, $e_k^{t_i} \sim N(\phi_k^t, \hat{\sigma}_{e_k: t_i}^2)$, with $\hat{\sigma}_{e_k: t_i}^2 = [S_k|_{k-1}]_{33}$.

- **False Target.** The bearing of a false-target measurement, $b_k^{f t_i}$, has a Gaussian distribution with mean θ_k^t and variance $\hat{\sigma}_{b_k: f t_i}^2$, where $\hat{\sigma}_{b_k: f t_i}^2$ is the same as the value in (5). Notice that the mean value is the *target*, hence the false target is (on average) aligned with the true target. This model inherently assumes that no angle ECM is being used, which is reasonable for monopulse radars such as the Benchmark Radar. Against monopulse radars creation of angle false targets is difficult and requires polarization ECM, which can only be generated by a few sophisticated ECM systems. The elevation model for a false-target measurement follows an identical model, $e_k^{f t_i} \sim N(\phi_k^t, \hat{\sigma}_{e_k: f t_i}^2)$.
- **Clutter.** Clutter returns occur when radar energy scatters off of objects in the field of view that are *not* of interest (e.g., land, water, buildings, etc.). Since the placement of clutter objects within the radar beam is random, a uniform distribution across the beam is a reasonable assumption. The Benchmark 2 Problem does not include clutter returns, therefore we will not consider this measurement type in our performance study.

4.2. Hypotheses

The hypothesis that RGPO is present and a target-FT measurement pair exists is based on the bearing and elevation differences among the received measurements

$$\Delta b_k^{ij} = b_k^i - b_k^j, \quad \Delta e_k^{ij} = e_k^i - e_k^j \quad (6)$$

In a single-target environment, there are five possibilities (hypotheses) for the *common-angle measurements*: (a) a pure clutter pair (hypothesis H_{cc}); (b) a clutter and target measurement pair (H_{ct}); (c) a false-target measurement pair (including the cover pulse) or a target and false-target measurement pair (H_{tf}), both referred to as a *target-FT* measurement pair; (d) a multiple false-target measurement pair, excluding the cover pulse (H_{ff}); and (e) a clutter and false-target measurement pair (H_{cf}). This formulation is general in that it is applicable for tracking in the presence of all range deception ECMs including range-gate-pull-in and range false targets. However, the focus for this paper is on the RGPO case only.

With these assumptions, the hypotheses mathematically become

$$H_{cc} : f(\Delta b_k^{ij}, \Delta e_k^{ij} | H_{cc}) = f_{cc}(\Delta b_k^{ij}, \Delta e_k^{ij}) \quad (7)$$

$$H_{ct} : f(\Delta b_k^{ij}, \Delta e_k^{ij} | H_{ct}) = f_{ct}(\Delta b_k^{ij}, \Delta e_k^{ij}) \quad (8)$$

$$H_{tf} : f(\Delta b_k^{ij}, \Delta e_k^{ij} | H_{tf}) = f_{tf}(\Delta b_k^{ij}, \Delta e_k^{ij}) \quad (9)$$

$$H_{ff} : f(\Delta b_k^{ij}, \Delta e_k^{ij} | H_{ff}) = f_{ff}(\Delta b_k^{ij}, \Delta e_k^{ij}) \quad (10)$$

4.2.1. Density function for a clutter-clutter pair

Hypothesis H_{cc} actually consists of three sub-hypotheses H'_{cc} (a clutter return pair), H''_{cc} (a clutter return and a false alarm), and H'''_{cc} (a false alarm pair). The complete density function for these sub-hypotheses is given in our first paper.¹ Since the Benchmark 2 Problem does not include clutter returns, we may simplify the function $f_{cc}(\Delta b_k^{ij}, \Delta e_k^{ij})$ to include only the false alarms,

$$f_{cc}(\Delta b_k^{ij}, \Delta e_k^{ij}) = N(\Delta b_k^{ij}; 0, \hat{\sigma}_{b_k:f a_i}^2 + \hat{\sigma}_{b_k:f a_j}^2) \cdot N(\Delta e_k^{ij}; 0, \hat{\sigma}_{e_k:f a_i}^2 + \hat{\sigma}_{e_k:f a_j}^2) \quad (11)$$

Here, the means are zero because $E\{b_k^{f a_i}\} - E\{b_k^{f a_j}\} = \hat{b}_k - \hat{b}_k = 0$ and $E\{e_k^{f a_i}\} - E\{e_k^{f a_j}\} = \hat{e}_k - \hat{e}_k = 0$.

4.2.2. Density function for a target-FT pair

Hypothesis H_{tf} actually consists of two sub-hypotheses: H'_{tf} (a target and false-target measurement pair) and H''_{tf} (a false-target pair, one being the cover pulse). Accordingly, the function $f_{tf}(\Delta b_k^{ij}, \Delta e_k^{ij})$ is given by

$$\begin{aligned} f_{tf}(\Delta b_k^{ij}, \Delta e_k^{ij}) &= N(\Delta b_k^{ij}; 0, \hat{\sigma}_{b_k:t_i}^2 + \hat{\sigma}_{b_k:f t_j}^2) \cdot N(\Delta e_k^{ij}; 0, \hat{\sigma}_{e_k:t_i}^2 + \hat{\sigma}_{e_k:f t_j}^2) P\{H'_{tf} | H_{tf}\} \\ &+ N(\Delta b_k^{ij}; 0, \hat{\sigma}_{b_k:f t_i}^2 + \hat{\sigma}_{b_k:f t_j}^2) \cdot N(\Delta e_k^{ij}; 0, \hat{\sigma}_{e_k:f t_i}^2 + \hat{\sigma}_{e_k:f t_j}^2) P\{H''_{tf} | H_{tf}\} \end{aligned} \quad (12)$$

$$\approx N(\Delta b_k^{ij}; 0, \hat{\sigma}_{b_k:f t_i}^2 + \hat{\sigma}_{b_k:f t_j}^2) \cdot N(\Delta e_k^{ij}; 0, \hat{\sigma}_{e_k:f t_i}^2 + \hat{\sigma}_{e_k:f t_j}^2) \quad (13)$$

The approximation holds because $P\{H'_{tf} | H_{tf}\} \approx 1$ since the cover pulse rather than the skin return is usually detected. Moreover, $\hat{\sigma}_{b_k:t_i}^2 \approx \hat{\sigma}_{b_k:f t_i}^2$ and $\hat{\sigma}_{e_k:t_i}^2 \approx \hat{\sigma}_{e_k:f t_i}^2$ in most circumstances. As a result, $f(\Delta b_k^{ij}, \Delta e_k^{ij} | H_{tf}) \approx f(\Delta b_k^{ij} | H_{ff})$ and thus we merge H_{ff} into H_{tf} . The mean values in (12) are zero because $E\{b_k^{t_i}\} - E\{b_k^{f t_j}\} = \theta_k^t - \theta_k^t = 0$ and $E\{e_k^{t_i}\} - E\{e_k^{f t_j}\} = \phi_k^t - \phi_k^t = 0$. Also, we have made use of the fact that the true target is always assumed to be closer than the false target, ($r_k^i < r_k^j$), therefore it is not necessary to consider the alternate combinations of target and false alarm $\hat{\sigma}_{b_k}^2$ values in the density function.

4.2.3. Density function for a clutter-target pair

The function $f_{ct}(\Delta b_k^{ij}, \Delta e_k^{ij})$ is given by

$$f_{ct}(\Delta b_k^{ij}, \Delta e_k^{ij}) = N(\Delta b_k^{ij}; 0, \hat{\sigma}_{b_k:ct}^2) \cdot N(\Delta e_k^{ij}; 0, \hat{\sigma}_{e_k:ct}^2) \quad (14)$$

where

$$\hat{\sigma}_{b_k:ct}^2 = \left(\hat{\sigma}_{b_k:t_i}^2 + \hat{\sigma}_{b_k:fa_j}^2 \right) P\{z_k^{t_i}, z_k^{fa_j} | z_k^i, z_k^j\} + \left(\hat{\sigma}_{b_k:fa_i}^2 + \hat{\sigma}_{b_k:t_j}^2 \right) P\{z_k^{fa_i}, z_k^{t_j} | z_k^i, z_k^j\} \quad (15)$$

$$\hat{\sigma}_{e_k:ct}^2 = \left(\hat{\sigma}_{e_k:t_i}^2 + \hat{\sigma}_{e_k:fa_j}^2 \right) P\{z_k^{t_i}, z_k^{fa_j} | z_k^i, z_k^j\} + \left(\hat{\sigma}_{e_k:fa_i}^2 + \hat{\sigma}_{e_k:t_j}^2 \right) P\{z_k^{fa_i}, z_k^{t_j} | z_k^i, z_k^j\} \quad (16)$$

In this density expression, $P\{z_k^{t_i}, z_k^{fa_j} | z_k^i, z_k^j\}$ is the probability that z_k^i is the target while z_k^j is the false alarm, while $P\{z_k^{fa_i}, z_k^{t_j} | z_k^i, z_k^j\}$ is the probability of the opposite condition. Since the SNR is a good indicator of which measurement is the target (i.e., the stronger one), we can approximate these probabilities in the following way:

$$P\{z_k^{t_i}, z_k^{fa_j} | z_k^i, z_k^j\} \approx \frac{\hat{\mathfrak{R}}_k^i}{\hat{\mathfrak{R}}_k^i + \hat{\mathfrak{R}}_k^j}, \quad P\{z_k^{fa_i}, z_k^{t_j} | z_k^i, z_k^j\} \approx \frac{\hat{\mathfrak{R}}_k^j}{\hat{\mathfrak{R}}_k^i + \hat{\mathfrak{R}}_k^j} \quad (17)$$

Notice that the mean values for the density are zero, $E\{b_k^{t_i}\} - E\{b_k^{fa_j}\} = E\{\theta_k^t\} - \hat{b}_k = 0$, since the prior estimate of the true target bearing is the beam boresight.

4.3. Hypothesis test for detection of common angle measurements

To detect the presence of RGPO, we form the *null hypothesis*, H_0 , that z_k^i and z_k^j is **not** a target-FT measurement pair, i.e.,

$$H_0 : f(\Delta b_k^{ij}, \Delta e_k^{ij} | H_0) \neq f_{tf}(\Delta b_k^{ij}, \Delta e_k^{ij}) \quad (18)$$

The *alternative hypothesis*, $H_1 = H_{tf}$, is that the measurements do form a target-FT pair,

$$H_1 : f(\Delta b_k^{ij}, \Delta e_k^{ij} | H_1) = f_{tf}(\Delta b_k^{ij}, \Delta e_k^{ij}) \quad (19)$$

Since H_{cf} is dropped and H_{ff} is merged into H_{tf} , H_{cc} and H_{ct} form a partition of H_0 for the single-target case under consideration. By the total probability theorem, we have

$$f(\Delta b_k^{ij}, \Delta e_k^{ij} | H_0) = f(\Delta b_k^{ij}, \Delta e_k^{ij} | H_{cc})P\{H_{cc}|H_0\} + f(\Delta b_k^{ij}, \Delta e_k^{ij} | H_{ct})P\{H_{ct}|H_0\} \quad (20)$$

where $P\{H_{cc}|H_0\}$ and $P\{H_{ct}|H_0\}$ are given by (35)–(36) below.

Given two measurements with a small bearing and elevation differences, Δb_k^{ij} and Δe_k^{ij} , and using the density functions defined in (19) and (20), we perform the following optimum **joint likelihood ratio test**:

- Decide on H_0 (i.e., reject z_k^i and z_k^j as a target-FT measurement pair) if

$$L_k^{ij} = \frac{f(\Delta b_k^{ij}, \Delta e_k^{ij} | H_1)}{f(\Delta b_k^{ij}, \Delta e_k^{ij} | H_0)} < \lambda \quad (21)$$

- Decide on H_1 (i.e., accept z_k^i and z_k^j as a target-FT measurement pair) if $L_k^{ij} > \lambda$. If H_1 is not accepted for any pair of measurements with “common” angles in the track gate, it is deemed that there are no range deception measurements in the radar dwell.
- A so-called randomized test can be conducted to decide on H_0 or H_1 if $L_k^{ij} = \lambda$, which is omitted here since $L_k^{ij} = \lambda$ has zero probability of occurrence for our problem.

In the likelihood ratio test the threshold λ is a scalar constant that is determined from the maximum allowable type I error probability α ,

$$P\{L_k^{ij} > \lambda | H_0\} = \alpha \quad (22)$$

Typically, we choose a small value for α , say 0.05. The value of λ is computed as follows. Let $\hat{\sigma}_{b_1}^2 = \hat{\sigma}_{b_k:ft_i}^2 + \hat{\sigma}_{b_k:ft_j}^2$ and $\hat{\sigma}_{e_1}^2 = \hat{\sigma}_{e_k:ft_i}^2 + \hat{\sigma}_{e_k:ft_j}^2$. Also, use $\hat{\sigma}_{b_0}^2 = \hat{\sigma}_{b_k:ct}^2$ defined in (15) and $\hat{\sigma}_{e_0}^2 = \hat{\sigma}_{e_k:ct}^2$ as in (16). Then the likelihood

ratio test can be expressed as

$$\begin{aligned}
L_k^{ij} &= \frac{N(\Delta b_k^{ij}; 0, \hat{\sigma}_{b1}^2) \cdot N(\Delta e_k^{ij}; 0, \hat{\sigma}_{e1}^2)}{N(\Delta b_k^{ij}; 0, \hat{\sigma}_{b0}^2) \cdot N(\Delta e_k^{ij}; 0, \hat{\sigma}_{e0}^2)} \\
&= \frac{(2\pi\hat{\sigma}_{b1}^2)^{-1/2} \exp\left(-(\Delta b_k^{ij})^2/2\hat{\sigma}_{b1}^2\right) \cdot (2\pi\hat{\sigma}_{e1}^2)^{-1/2} \exp\left(-(\Delta e_k^{ij})^2/2\hat{\sigma}_{e1}^2\right)}{(2\pi\hat{\sigma}_{b0}^2)^{-1/2} \exp\left(-(\Delta b_k^{ij})^2/2\hat{\sigma}_{b0}^2\right) \cdot (2\pi\hat{\sigma}_{e0}^2)^{-1/2} \exp\left(-(\Delta e_k^{ij})^2/2\hat{\sigma}_{e0}^2\right)} \\
&= c_0 \exp\left(-\frac{(\Delta b_k^{ij})^2 c_1}{\hat{\sigma}_{b0}^2}\right) \cdot \exp\left(-\frac{(\Delta e_k^{ij})^2 c_2}{\hat{\sigma}_{e0}^2}\right) > \lambda
\end{aligned} \tag{23}$$

where

$$c_0 = \left(\frac{\hat{\sigma}_{b0}^2 \hat{\sigma}_{e0}^2}{\hat{\sigma}_{b1}^2 \hat{\sigma}_{e1}^2}\right)^{1/2}, \quad c_1 = \frac{\hat{\sigma}_{b0}^2 - \hat{\sigma}_{b1}^2}{2\hat{\sigma}_{b1}^2}, \quad c_2 = \frac{\hat{\sigma}_{e0}^2 - \hat{\sigma}_{e1}^2}{2\hat{\sigma}_{e1}^2} \tag{24}$$

From this expression, the log-likelihood ratio may be computed as

$$\ln(L_k^{ij}) = \ln(c_0) - \frac{(\Delta b_k^{ij})^2 c_1}{\hat{\sigma}_{b0}^2} - \frac{(\Delta e_k^{ij})^2 c_2}{\hat{\sigma}_{e0}^2} > \ln(\lambda) \tag{25}$$

Equation (25) can be expressed as

$$\frac{(\Delta b_k^{ij})^2 c_1}{\hat{\sigma}_{b0}^2} + \frac{(\Delta e_k^{ij})^2 c_2}{\hat{\sigma}_{e0}^2} < \ln(c_0) - \ln(\lambda) \tag{26}$$

Recall from (22) that we evaluate the probability under the condition that the null hypothesis is true, thus $\Delta b_k^{ij} \sim N(0, \hat{\sigma}_{b0}^2)$ and $\Delta e_k^{ij} \sim N(0, \hat{\sigma}_{e0}^2)$. Therefore, $(\Delta b_k^{ij})^2/\hat{\sigma}_{b0}^2$ and $(\Delta e_k^{ij})^2/\hat{\sigma}_{e0}^2$ are Chi-square distributed random variables. Since the left-hand side of this expression represents the weighted sum of two independent Chi-square random variables, we can compute the density function and evaluate the probability that it is less than the right-hand side. This is the optimal approach for computation of the threshold, but it is complicated. A second possible (and simpler) approach is to use the moment matching technique shown in Section 1.4.18 of Ref. 8. A third (and simplest) approach is to make one assumption, $c_1 \approx c_2$, which is usually the case. Then, the left hand side of the expression

$$\frac{(\Delta b_k^{ij})^2}{\sigma_{b0}^2} + \frac{(\Delta e_k^{ij})^2}{\sigma_{e0}^2} \begin{cases} < \frac{\ln(c_0) - \ln(\lambda)}{c_1}, & c_1 > 0 \\ > \frac{\ln(c_0) - \ln(\lambda)}{c_1}, & c_1 < 0 \end{cases} \tag{27}$$

is a Chi-square random variable with two degrees of freedom. For a Chi-square random variable χ^2 , the probability that the random variable exceeds the statistic $\chi_{\alpha,n}^2$ is $P\{\chi^2 \geq \chi_{\alpha,n}^2\} = \alpha$, where $\chi_{\alpha,n}^2$ is obtained from a Chi-square table. An equivalent expression is $P\{\chi^2 < \chi_{1-\alpha,n}^2\} = \alpha$. Since we found in (27) that (22) could be approximated as

$$P\{L_k^{ij} > \lambda | H_0\} \approx \begin{cases} P\left\{(\Delta b_k^{ij})^2/\sigma_{b0}^2 + (\Delta e_k^{ij})^2/\sigma_{e0}^2 < [\ln(c_0) - \ln(\lambda)]/c_1\right\} = \alpha, & c_1 > 0 \\ P\left\{(\Delta b_k^{ij})^2/\sigma_{b0}^2 + (\Delta e_k^{ij})^2/\sigma_{e0}^2 > [\ln(c_0) - \ln(\lambda)]/c_1\right\} = \alpha, & c_1 < 0 \end{cases} \tag{28}$$

then the threshold can be determined from the two cases for the Chi-square statistic,

$$\lambda = \begin{cases} c_0 \exp(-c_1 \cdot \chi_{1-\alpha,2}^2), & c_1 > 0 \\ c_0 \exp(-c_1 \cdot \chi_{\alpha,2}^2), & c_1 < 0 \end{cases} \tag{29}$$

The *detection* of common angle measurements is conducted by identifying any measurement pairs for which $L_k^{ij} > \lambda$. If more than one pair exceeds the threshold, several approaches are possible. Since we know that in the Benchmark 2 Problem that only one target and one false target can be present at a time, we may retain only the *most likely* target-FT pair. Hence, we identify the target-FT pair as the one that gives $\max(L_k^{ij})$.

4.4. Calculation of the prior probabilities

Let the angle (bearing and elevation) beamwidth at time k be $[B_k^b, B_k^e]$. Then the equivalent number of angle cells, N_k , associated with an accepted common-angle measurement pair is given by the smallest integer that is not smaller than $(B_k^b/|\Delta b_k^{ij}|)(B_k^e/|\Delta e_k^{ij}|)$; that is, $N_k = \lceil B_k^b/|\Delta b_k^{ij}| \rceil \lceil B_k^e/|\Delta e_k^{ij}| \rceil$.

The prior probability that a given accepted pair of common-angle measurements is formed by pure clutter measurements (in a given angle cell) is given by the binomial distribution over the M range cells,

$$P\{H_{cc}\} = p_{cc} = \binom{M}{2} (P_c^{ij})^2 (1 - P_c^{ij})^{M-2} \quad (30)$$

where

$$P_c^{ij} = P_{fa} \cdot \frac{\operatorname{erf}\left(\frac{\sqrt{2}(\hat{b}_k - b_k^i)}{2\hat{\sigma}_{b_k:fa_{ij}}}\right) - \operatorname{erf}\left(\frac{\sqrt{2}(\hat{b}_k - b_k^j)}{2\hat{\sigma}_{b_k:fa_{ij}}}\right)}{\operatorname{erf}\left(\frac{\sqrt{2}B_k^b}{4\hat{\sigma}_{b_k:fa_{ij}}}\right) - \operatorname{erf}\left(\frac{-\sqrt{2}B_k^b}{4\hat{\sigma}_{b_k:fa_{ij}}}\right)} \cdot \frac{\operatorname{erf}\left(\frac{\sqrt{2}(\hat{e}_k - e_k^i)}{2\hat{\sigma}_{e_k:fa_{ij}}}\right) - \operatorname{erf}\left(\frac{\sqrt{2}(\hat{e}_k - e_k^j)}{2\hat{\sigma}_{e_k:fa_{ij}}}\right)}{\operatorname{erf}\left(\frac{\sqrt{2}B_k^e}{4\hat{\sigma}_{e_k:fa_{ij}}}\right) - \operatorname{erf}\left(\frac{-\sqrt{2}B_k^e}{4\hat{\sigma}_{e_k:fa_{ij}}}\right)} \quad (31)$$

and $\hat{\sigma}_{b_k:fa_{ij}} = (\hat{\sigma}_{b_k:fa_i}^2/2 + \hat{\sigma}_{b_k:fa_j}^2/2)^{1/2}$.

The prior probability that a given accepted pair of common-angle measurements is formed by one target and one clutter measurements is given by

$$P\{H_{ct}\} = p_{ct} = 2 \frac{P_d P_g}{NM} \binom{M-1}{1} (P_{fa}/N)(1 - P_{fa}/N)^{M-2} \quad (32)$$

where P_d and P_g are the target detection probability and the track gate probability, respectively. This formula follows from the fact that a target-clutter measurement pair will be accepted if and only if the target is detected; its measurement falls inside the given angle cell of the gate; *and* the clutter measurement falls within the same angle cell but in range cells distinct from each other and from the target measurement.

Since H_{cf} is neglected and H_{ff} is merged into H_{tf} , the prior probability that a given accepted pair of common-angle measurements is formed by one target measurement (or cover pulse measurement) and one false-target measurement is given by

$$P\{H_{tf}\} = p_{tf}^{ij} = 2 \left(\frac{P'_d P_g}{NM} \right) \cdot P_{tf}^{ij} \quad (33)$$

where the probability of detecting a false target is $P'_d \approx 1$. The prior probability that a false target is in the (i, j) th angle cell is

$$P_{tf}^{ij} = P'_d \cdot \operatorname{erf}\left(\frac{\sqrt{2}|\Delta b_k^{ij}|}{4\sqrt{(\sigma_{b_k:ft_i}^2 + \sigma_{b_k:ft_j}^2)/2}}\right) \cdot \operatorname{erf}\left(\frac{\sqrt{2}|\Delta e_k^{ij}|}{4\sqrt{(\sigma_{e_k:ft_i}^2 + \sigma_{e_k:ft_j}^2)/2}}\right) \quad (34)$$

The conditional probabilities in (20) are given by

$$P\{H_{cc}|H_0\} = \frac{P\{H_{cc}\}}{P\{H_0\}} = \frac{p_{cc}}{p_{cc} + p_{ct}} = \left[1 + \frac{4P_d P_g}{M^2 P_{fa}}\right]^{-1} \quad (35)$$

$$P\{H_{ct}|H_0\} = \frac{P\{H_{ct}\}}{P\{H_0\}} = \frac{p_{ct}}{p_{cc} + p_{ct}} = \left[\frac{4P_d P_g}{M^2 P_{fa}}\right] \left[1 + \frac{4P_d P_g}{M^2 P_{fa}}\right]^{-1} \quad (36)$$

From these prior probabilities of the hypotheses, we may compute the posterior probabilities

$$P\{H_\ell|Z_k\} \approx P\{H_\ell|\Delta b_k^{ij}, \Delta e_k^{ij}\} = \frac{f(\Delta b_k^{ij}, \Delta e_k^{ij}|H_\ell)}{f(\Delta b_k^{ij}, \Delta e_k^{ij})} P\{H_\ell\} \quad (37)$$

where $f(\Delta b_k^{ij}, \Delta e_k^{ij}|H_\ell)$ was given in (19) and (20), and

$$f(\Delta b_k^{ij}, \Delta e_k^{ij}) = f(\Delta b_k^{ij}, \Delta e_k^{ij}|H_0)P\{H_0\} + f(\Delta b_k^{ij}, \Delta e_k^{ij}|H_1)P\{H_1\} \quad (38)$$

5. TRACKING, DATA ASSOCIATION AND FUSION

5.1. Common angle target-FT tracker

We use a conventional constant velocity extended Kalman filter (EKF) to track the target using the measurements identified as the target-FT pair. The unique aspect of the tracker is the fact that there are two sets of measurements of the target bearing and elevation. One set is from the true target return and the other is from the RGPO false target. We combine the two sets in the tracker to take advantage of the extra information.

In the Benchmark 2 Problem, only single false target RGPO programs are implemented. For simplicity we will assume only one target-FT pair is possible (but the methodology is extended to multiple false targets¹). Without loss of generality, let z_k^1 and z_k^2 denote two common angle measurements identified by the hypothesis test. A new measurement is formed by combining the bearing and elevation of the farthest target,

$$z_k^* = [\min(r_k^1, r_k^2) \quad b_k^1 \quad e_k^1 \quad b_k^2 \quad e_k^2]'$$
 (39)

The closest measurement in range is assumed to be the true target since the ECM system in the Benchmark 2 Problem is known to only produce range-trailing RGPO false targets.

Given the extension to the measurement vector, we must modify definitions in the EKF. The transformation $z_k^* = h(x_k)$ must be redefined to duplicate the bearing and elevation in the fourth and fifth elements of z_k^* . Similarly, the Jacobian matrix H_k in the EKF is redefined to be a 5×6 matrix, where the second and third rows are repeated in the fourth and fifth rows. Also, the measurement covariance matrix is redefined as $R_k = \text{diag}[\sigma_{r_k}^2 \quad \sigma_{b_k}^2 \quad \sigma_{e_k}^2 \quad \sigma_{b_k}^2 \quad \sigma_{e_k}^2]$.

The state and covariance estimates of the target (using the common angle measurements) are formed from the fused predicted state and covariance $(x_{k|k-1}, P_{k|k-1})$ and z_k^* ,

$$\hat{x}_{k|k}^{(1)} = \hat{x}_{k|k-1} + K_k(z_k^* - h(\hat{x}_{k|k-1}))$$
 (40)

$$P_{k|k}^{(1)} = (I - K_k H_k) P_{k|k-1}$$
 (41)

where K_k is the Kalman gain in the EKF.

5.2. Tracking with the remaining measurements

The second component to the tracking is to run a conventional tracking-in-clutter filter on the partition of measurements that remain after the target-FT measurements have been separated. The idea with this filter is to provide a secondary method that will “catch” any target measurements that might be missed by the common angle hypothesis test.

We considered two different tracking-in-clutter filters for this application: the Strongest Neighbor (SN) filter and the Probabilistic Data Association (PDA) filter. We assessed the performance of both using the spherical measurement coordinate frame with the EKF. The SN data association approach is very simple. When we receive a collection of measurements, we identify the one with the largest SNR (the strongest). That measurement is assigned to be the one used in the EKF state estimate and covariance update. The approach is very effective when the target SNR is typically greater than that for false alarms or clutter. But in the presence of ECM, it can be very vulnerable. But in principle our hypothesis test removes all ECM measurements into a separate partition, hence the SN filter should be very effective for tracking using only the remaining measurements.

The PDA filter⁸ state estimate is computed from the weighted sum of the state estimates formed using the validated measurements,

$$\hat{x}_{k|k}^{(0)} = \sum_{i=0}^{m_k} \beta_k^i \hat{x}_{k|k}^i$$
 (42)

where $\hat{x}_{k|k}^i$ is the updated state conditioned on the i th measurement in the validated set,

$$\hat{x}_{k|k}^i = \hat{x}_{k|k-1} + K_k(z_k^i - \hat{z}_k)$$
 (43)

The Kalman gain K_k is computed in the usual way. The weight β_k^i is the conditional probability of the i th validated measurement being the correct one for association. The covariance update incorporates uncertainty in the measurement origin and is computed as

$$P_{k|k}^{(0)} = \beta_k^0 P_{k|k-1} + (1 - \beta_k^0) P_{k|k}^c + \tilde{P}_{k|k} \quad (44)$$

In this expression, there are three components to the covariance update calculation. The first term on the right-hand side, $\beta_k^0 P_{k|k-1}$, accounts for the possibility that the true measurement is not in the gate. The second term, $(1 - \beta_k^0) P_{k|k}^c$, is the weighted covariance for the correct measurement. The third term is called the ‘‘spread of the innovations term.’’ It increases the covariance, and it comes about because of the measurement origin uncertainty in the collection of validated measurements.

5.3. Fusion of two tracks

The final step is to form a fused estimate for the target using both partitions of measurements. Several approaches are possible. The one we used is to form a probabilistically weighted sum of estimates from the tracking algorithms as

$$\hat{x}_{k|k} = \hat{x}_{k|k}^{(0)} P\{H_0|Z_k\} + \hat{x}_{k|k}^{(1)} P\{H_1|Z_k\} \quad (45)$$

Similarly, the covariance is computed to be

$$\begin{aligned} P_{k|k} &= P_{k|k}^{(0)} P\{H_0|Z_k\} + P_{k|k}^{(1)} P\{H_1|Z_k\} \\ &+ (\hat{x}_{k|k} - \hat{x}_{k|k}^{(0)})(\hat{x}_{k|k} - \hat{x}_{k|k}^{(0)})' P\{H_0|Z_k\} + (\hat{x}_{k|k} - \hat{x}_{k|k}^{(1)})(\hat{x}_{k|k} - \hat{x}_{k|k}^{(1)})' P\{H_1|Z_k\} \end{aligned} \quad (46)$$

6. EVALUATION OF THE DECOMPOSITION AND FUSION TECHNIQUE

6.1. Model parameters

We utilized the Benchmark 2 Problem simulation for evaluation and comparison of the D&F-ARGPO technique. The Benchmark 2 Problem requires that the tracking algorithm perform resource allocation and adaptive dwell scheduling. It also includes a selectable RGPO waveform (linear or parabolic walk off). For the evaluation, we held all the other adaptive processes (other than data association) in the Benchmark 2 simulation constant. This allowed for direct comparison of the tracking performance without having to interpret/compensate for other processing factors. We held the waveform number constant throughout the simulation; we set it to waveform #5, which has the best combination of range resolution (22.5 m) and expected SNR (11.3 dB for a 1.0 m² target at 100 km). We held the radar revisit time constant at 0.5 sec. After a missed detection, the revisit time was set to 0.1 sec. No special reacquisition logic was applied. We used the linear walk-off program for the false target with a rate of $v_0 = 100$ m/s. The process noise covariance matrix in the constant velocity filter was set to $Q = 60I$.

One other note is that for this assessment we used prior variance values instead of posterior values for $\hat{\sigma}_{b_k:fa_i}^2$, $\hat{\sigma}_{e_k:fa_i}^2$, $\hat{\sigma}_{b_k:ti}^2$, and $\hat{\sigma}_{e_k:ti}^2$. That is, we used fixed values determined from data collected over a number of Monte Carlo runs instead of the values reported by the radar. We did this because it added some robustness to the decomposition procedure. In the future, we expect to improve the algorithm and use the reported (posterior) variance values instead.

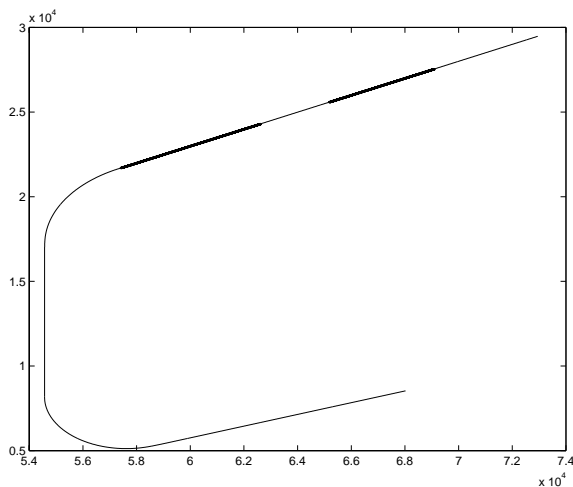
6.2. Simulation results

To evaluate the tracking performance we conducted a simulation using 100 Monte Carlo trials. We used the Target-1 scenario, which is shown in Figure 1a. Notice that the RGPO is turned on only during portions of the scenario: during the 15-30 sec interval, and during the 40-60 sec interval. The lost-track results are shown in Table 1 for the four different tracking algorithms. The first two columns show the percent lost without and with the RGPO turned on. The last three columns break the lost track percentage within three sets of time values: during RGPO, immediately after RGPO (15 sec interval following completion of the RGPO), and otherwise.

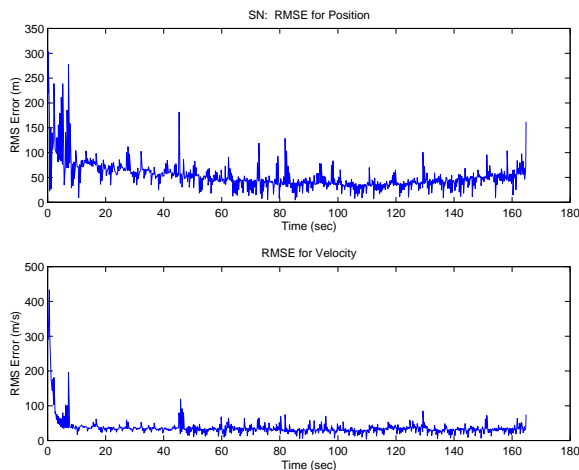
The results show that standard tracking techniques (strongest neighbor, nearest neighbor, and PDAF) track the target very well in a non-ECM environment, as the track loss percent is very low (2% or less). Further, Figure 1b shows that for the Strongest Neighbor filter that the tracking error is small (about 50 m) during the ECM-off scenario. But when the RGPO ECM is on, the track loss percent is very high (86-94%), indicating that the three methods are all very vulnerable to the RGPO. The third and fourth columns in Table 1 show that most of the tracks

Table 1. Lost target performance for Target-1.

Technique	% Lost Tracks		% Lost During RGPO	% Lost After RGPO	% Lost Other
	RGPO-off	RGPO-on			
Strongest Neighbor	0	94	4	61	29
Nearest Neighbor	2	86	13	60	13
PDAF	1	91	16	51	24
D&F-ARGPO(SN)	0	34	3	26	5



(a) Target-1 scenario with ECM on highlighted.



(b) SN RMSE, ECM off.

Figure 1. Target-1, (a) scenario, and (b) Strongest Neighbor position/velocity RMSE with ECM off.

are lost during or shortly after the ECM-on periods. Figure 2a shows the Strongest Neighbor RMSE with ECM on. The impact of the ECM can be seen in the position error plot, where the linear walk-off is very visible. Figure 2b shows a histogram of the times when the track is lost; clearly, most occur during or near the ECM activation times. Similar plots for the Nearest Neighbor and PDA filters show that the ECM clearly has a strong influence on the tracking error.

The last row in Table 1 shows the tracking performance of the D&F-ARGPO filter. In this particular implementation we used the Strongest Neighbor filter to process all remaining measurements after target-FT pairs have been removed. Also, to reduce cases of false identification of target-FT pairs, we added a SNR threshold criteria to the likelihood ratio test: only pairs with an SNR greater than 10 dB were considered as target-FT pairs (we expect to make SNR part of the likelihood test in the future). With ECM off, the track lost percent was 0% showing that the RGPO-reject logic does not degrade the tracking. When ECM is on, the track loss percent is 34% showing that we have achieved significant improvement over the other techniques. However, 26% of the tracks were lost after the ECM activation period. Analysis of the tracking data showed that for the current implementation of the likelihood ratio test, a significant number of *missed detections* occur. Therefore, the ECM degraded the tracking in some instances. Figure 3a shows a plot of the RMSE performance, while Figure 3b shows the histogram of the number of track losses versus time. The plots confirm that tracking errors (and track loss) are reduced during the ECM activation times compared to the other methods, but errors (and track loss) shortly after the activation time are high. Our conclusion about these results is that RGPO rejection performance is encouraging but not up to our expectations. We believe that with further modifications of the model that we can reduce the number of missed detections and improve the performance. We expect to report this in the near future.

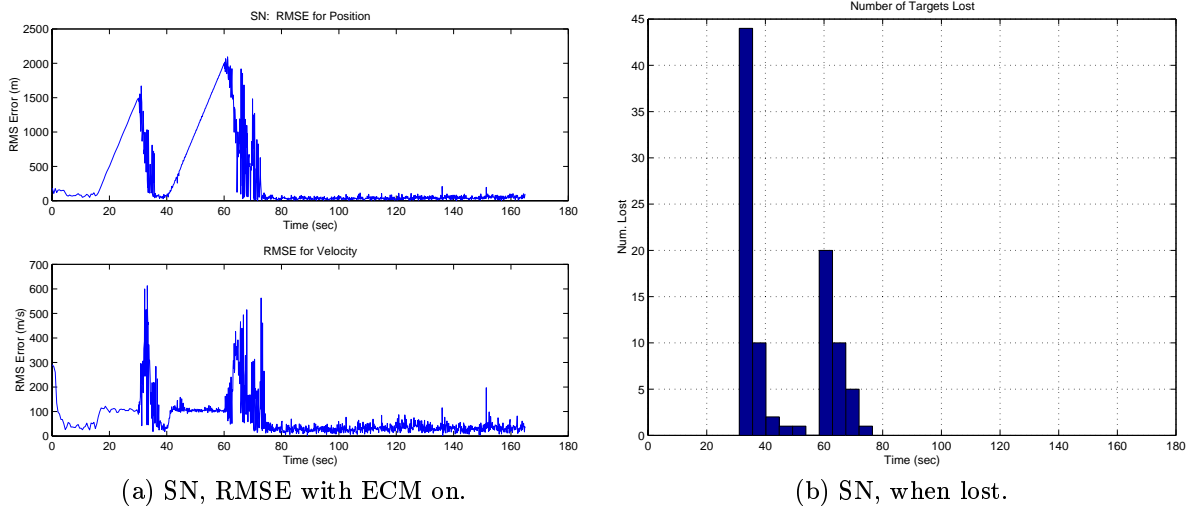


Figure 2. Target-1, (a) Strongest neighbor tracking performance, and (b) times when lost.

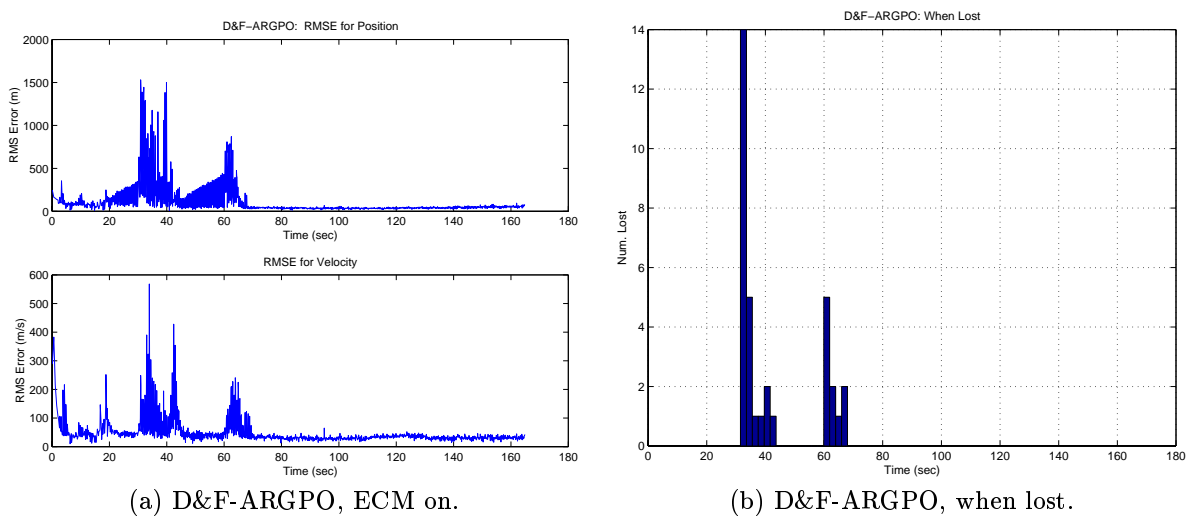


Figure 3. Target-1, (a) D&F-ARGPO filter with ECM on, and (b) histogram of lost tracks.

7. CONCLUSIONS

In this paper, we have presented a specific implementation of the general Decomposition and Fusion methodology¹ used to reject RGPO and range false target ECM techniques. The approach uses a hypothesis test to decompose a measurement set into target-FT pairs, and other measurements. Two tracking filters are subsequently run on the two measurements sets, and the results are fused together. Simulation results using the Benchmark 2 Problem environment showed that standard tracking techniques (Strongest Neighbor, Nearest Neighbor, and PDAF) are very vulnerable to the RGPO ECM. The D&F results showed that some improvement in tracking performance and rejection of the RGPO ECM, but we believe that better performance can be achieved with continued refinement of the approach. By including other features in the hypothesis test (e.g., range or measurement SNR), we believe that the performance of the test can be significantly improved.

REFERENCES

1. X. R. Li, B. J. Slocumb, and P. D. West, "Tracking in the presence of range deception ECM and clutter by decomposition and fusion," in *Signal and Data Processing of Small Targets 1999*, O. E. Drummond, ed., *Proceedings of the SPIE* **3809**, pp. 198–210, 1999.
2. W. D. Blair, G. A. Watson, G. L. Gentry, and S. Hoffman, "Benchmark problem for beam pointing control of phased array radar against maneuvering targets in the presence of ECM and false alarms," *Proceedings of the American Control Conference*, pp. 2601–2605, 1995.
3. W. D. Blair and G. A. Watson, "Benchmark problem for radar resource allocation and tracking maneuvering targets in the presence of ECM," Tech. Rep. NSWCCD/TR-96/10, Naval Surface Warfare Center, Dahlgren Division, September 1996.
4. W. D. Blair, G. A. Watson, T. Kirubarajan, and Y. Bar-Shalom, "Benchmark for radar allocation and tracking in ECM," *IEEE Transactions on Aerospace and Electronic Systems* **34**, pp. 1097–1114, October 1998.
5. T. Kirubarajan, Y. Bar-Shalom, and E. Daeipour, "Adaptive beam pointing control of a phased array radar in the presence of ECM and false alarms using IMM PDAF," *Proceedings of the American Control Conference*, pp. 2616–2620, 1995.
6. B. J. Slocumb and P. D. West, "ECM modeling for multitarget tracking and data association," in *Multitarget-Multisensor Tracking: Applications and Advances*, Y. Bar-Shalom and W. D. Blair, eds., ch. 8, Artech House, 2000.
7. W. D. Blair and M. Brandt-Pearce, "Statistical description of monopulse parameters for tracking Rayleigh targets," *IEEE Transactions on Aerospace and Electronic Systems* **34**, pp. 597–611, April 1998.
8. Y. Bar-Shalom and X. R. Li, *Estimation and Tracking: Principles, Techniques, and Software*, Artech House, Norwood, MA, 1993.